

## THE SUPERCAM REMOTE SENSING INSTRUMENT SUITE FOR MARS 2020

R.C. Wiens<sup>1</sup>, S. Maurice<sup>2</sup>, K. McCabe<sup>1</sup>, P. Cais<sup>3</sup>, R.B. Anderson<sup>4</sup>, O. Beyssac<sup>5</sup>, L. Bonal<sup>6</sup>, S. Clegg<sup>1</sup>, L. Deflores<sup>7</sup>, G. Dromart<sup>8</sup>, W.W. Fischer<sup>9</sup>, O. Forni<sup>2</sup>, O. Gasnault<sup>2</sup>, J.P. Grotzinger<sup>9</sup>, J.R. Johnson<sup>10</sup>, J. Martinez-Frias<sup>11</sup>, N. Mangold<sup>12</sup>, S. McLennan<sup>13</sup>, F. Montmessin<sup>14</sup>, F. Rull<sup>15</sup>, S.K. Sharma<sup>16</sup>, V. Sautter<sup>17</sup>, E. Lewin<sup>18</sup>, E. Cloutis<sup>19</sup>, F. Poulet<sup>20</sup>, S. Bernard<sup>17</sup>, T. McConnochie<sup>21</sup>, N. Lanza<sup>1</sup>, H. Newsom<sup>22</sup>, A. Ollila<sup>22</sup>, R. Leveille<sup>23</sup>, S. Le Mouelic<sup>12</sup>, J. Lasue<sup>2</sup>, N. Melikechi<sup>24</sup>, P.-Y. Meslin<sup>2</sup>, A. Misra<sup>16</sup>, O. Grasset<sup>12</sup>, S.M. Angel<sup>25</sup>, T. Fouchet<sup>26</sup>, P. Beck<sup>18</sup>, N. Bridges<sup>10</sup>, B. Bousquet<sup>3</sup>, C. Fabre<sup>27</sup>, P. Pinet<sup>2</sup>, K. Benzerara<sup>5</sup>, G. Montagnac<sup>8</sup> (<sup>1</sup>LANL, Los Alamos, NM; [rwuens@lanl.gov](mailto:rwuens@lanl.gov), <sup>2</sup>IRAP, Toulouse, France; <sup>3</sup>LAB <sup>4</sup>USGS; <sup>5</sup>IMPMC; <sup>6</sup>IPAG; <sup>7</sup>JPL; <sup>8</sup>PGLTPE; <sup>9</sup>Caltech; <sup>10</sup>APL/JHU; <sup>11</sup>CSIC-UCM; <sup>12</sup>LPG Nantes; <sup>13</sup>Stonybrook; <sup>14</sup>LATMOS; <sup>15</sup>UVA-CSIC; <sup>16</sup>U. Hawaii; <sup>17</sup>MNHN; <sup>18</sup>U. Grenoble; <sup>19</sup>U. Winnipeg; <sup>20</sup>IAS, U-Paris Sud; <sup>21</sup>GSFC; <sup>22</sup>UNM; <sup>23</sup>McGill; <sup>24</sup>DSU; <sup>25</sup>USC; <sup>26</sup>LESIA; <sup>27</sup>U. Nancy)

**Overview:** The Mars 2020 rover, essentially a structural twin of MSL, is being built to a) characterize the geology and history of a new landing site on Mars, b) find and characterize ancient habitable environments, c) cache samples for eventual return to Earth, and d) demonstrate in-situ production of oxygen needed for human exploration. Remote-sensing instrumentation is needed to support the first three of these goals [1]. The SuperCam instrument meets these needs with a range of instrumentation including the highest-resolution remote imaging on the rover, two different techniques for determining mineralogy, and one technique to provide elemental compositions. All of these techniques are co-observed, providing rapid comprehensive characterization. In addition, for targets within 7 meters of the rover the laser shock waves brush away the dust, providing cleaner surfaces for analysis. SuperCam will use an advanced version of the AEGIS robotic target selection software.

**Instrument Architecture:** SuperCam's overall design (Fig. 1) is strongly patterned after ChemCam, being divided into a Mast Unit (MU) and Body Unit (BU) with an optical fiber and electrical cables connecting the units. The MU includes a 110 mm telescope, a Nd:YAG laser (1064 & 532 nm beams), an IR spectrometer, the Remote Micro-Imager (RMI) camera, and associated electronics. The Body Unit consists of two reflection spectrometers of ChemCam heritage plus an all-purpose transmission spectrometer for laser-induced breakdown (LIBS), Raman, and VIS spectroscopy. The MU is built in France, while the BU is built at LANL. A set of rover calibration targets are being assembled in Spain.

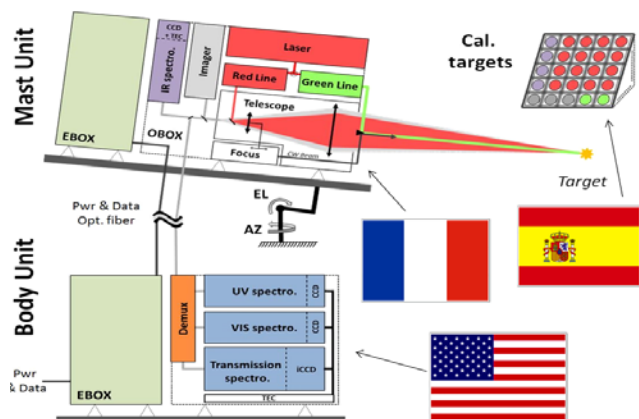


Fig. 1. SuperCam schematic diagram.

**Visible and Infrared (VISIR) Spectroscopy:** Mineralogy detection is performed by both Raman and VISIR reflectance spectroscopy. The VISIR spectral range extends from 0.4 to 2.6  $\mu\text{m}$  with two gaps, one at 0.47-0.54, and the other at 0.86-1.3  $\mu\text{m}$ . Spectrometers in the BU cover the range from 0.4-0.86  $\mu\text{m}$  at high spectral resolution, while the 1.3-2.6  $\mu\text{m}$  range is covered in 248 channels by a wavelength-scanning AOTF spectrometer in the MU [2]. The spectral resolution of the latter is 30  $\text{cm}^{-1}$  with sub-sampling to 15  $\text{cm}^{-1}$ . Fig. 2 shows a spectrum from the prototype spectrometer. A minimum signal-to-noise ratio of 45 is expected to be obtained within the required exposure times. Spatial resolution will be 0.8-1.1 mrad.

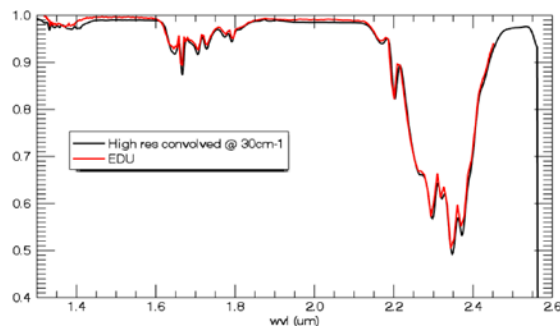


Fig. 2. Spectrum of CO gas cell with prototype SuperCam IR spectrometer.

**Raman Spectroscopy** is facilitated by frequency doubling the laser (532 nm Raman), adding a 532 nm notch filter, and detecting the Raman bands with a transmission spectrometer that replaces one of the ChemCam reflection spectrometers in the body. The miniature unit includes a flight-qualified intensifier that gates within 100 ns around the laser pulses, removing interfering fluorescence and ambient sunlight [e.g., 3]. Changing the start of the exposure relative to the laser allows studies of time-resolved fluorescence [4]. The Raman spectrometer is designed to observe olivine and brighter Raman-emitting minerals to a distance of 12 m with a field of view of 0.65 mrad (1.3 mm @ 2 m distance). This technique is highly complementary with VISIR spectroscopy, as Raman observes symmetric stretch bands generally not observed with VISIR, permitting easy identification of feldspars, an important component in Gale crater

mineralogy. An example spectrum from the prototype SuperCam Raman spectrometer [5] is shown in Fig. 3. The flight unit will have improved spectral resolution of  $10 \text{ cm}^{-1}$ .

**LIBS:** The ChemCam instrument has currently returned elemental compositions from more than 7,000 observation points in Gale crater (Fig. 4), demonstrating the important contribution of LIBS to planetary exploration. SuperCam will have a very similar LIBS capability to that of ChemCam, with observations to 7 m distance, and with spatial resolution of  $300\text{-}500 \mu\text{m}$  [6]. The LIBS will have a similar depth profiling capability, which on ChemCam has discovered thin layers of alteration (Li and other alkali elements [7] and Mn oxides [8].)

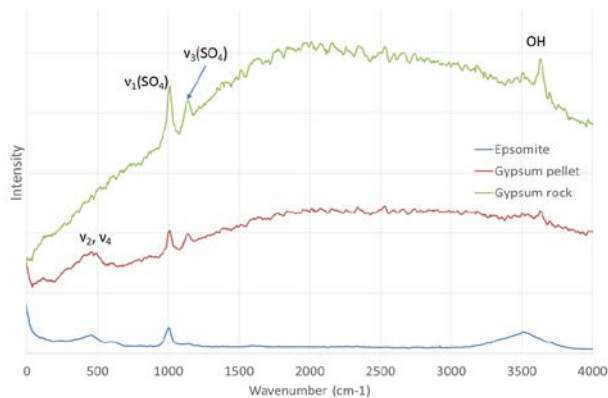


Fig. 3. Raman spectra from the SuperCam prototype transmission spectrometer. Spectra were obtained at 4 m distance using 1000 laser shots. The detector was exposed for a total of 100 s at room temperature to obtain these spectra. With the flight unit the CCD will be cooled and gated around the laser shots, greatly improving signal to noise.

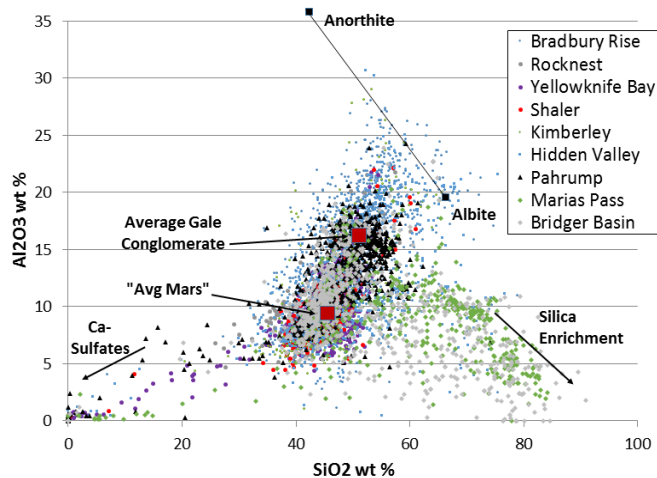


Fig. 4. ChemCam LIBS observations in Gale crater mapped distinct differences between regions. In coarse-grained rocks the compositions of pure minerals are obtained. SuperCam will have similar chemical mapping capabilities, co-aligned with Raman, VISIR, & RMI.

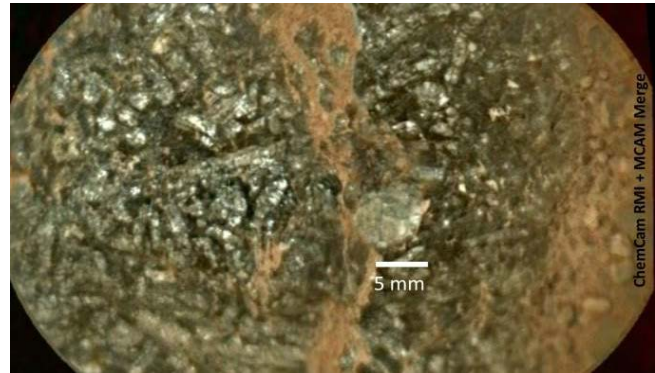


Fig. 5. Simulated SuperCam RMI mosaic made from a monochromatic ChemCam mosaic merged with Mastcam color. SuperCam will provide the highest resolution remote images on the Mars 2020 rover.

**RMI:** The RMI imager on SuperCam uses a CMOS detector with a Bayer color filter to provide the highest resolution remote images (e.g.,  $0.040 \text{ mrad}$  in a  $\sim 20 \text{ mrad}$  field of view, similar to ChemCam) in color [9]. These images use a high-dynamic-range compression to increase the intensity range using several exposures. The RMI detector and front-end electronics are encapsulated in a compact cube. A simulated image is shown in Fig. 5.

**Current Status:** SuperCam passed its preliminary design review in October and in 2016 it is proceeding with assembly and testing of the development unit, which will verify the Raman timing requirements and signal-to-noise ratios.

**Acknowledgement:** This work was supported by NASA's Mars Program Office in the US, by CNES in France, and by UVa-CSIC in Spain.

**References:** [1] Maurice S., et al. (2015) Lunar Planet Sci. XLVI, 2818; [2] Fouchet T. et al. (2015) Lunar Planet. Sci. XLVI, 1736; [3] Wiens R.C. et al. (2005) Spectrochim. Acta A61, 2324. [4] Sharma S.K. (2007) Spectrochim. Acta A68, 1008; [5] Clegg S. et al. (2015) Lunar Planet Sci XLVI, 2781; [6] Maurice et al., (2012) Spa. Sci. Rev. 170, 95; [7] Ollila et al. (2014) J. Geophys. Res., 119, 255; [8] Lanza et al. (2015) Lunar Planet. Sci. XLVI, 2893; and (2016) subm. to Geology. [9] Gasnault O. et al. (2015) Lunar Planet Sci. XLVI, 2990.